

ATCA^{*} H I Observations of the Peculiar Galaxy IC 2554

Bärbel Koribalski¹, Scott Gordon^{2,1}, Keith Jones²

¹*Australia Telescope National Facility, CSIRO, P.O. Box 76, Epping, NSW 1710, Australia; E-mail: Baerbel.Koribalski@csiro.au*

²*Department of Physics, University of Queensland, St. Lucia, Brisbane, QLD 4072, Australia*

Received date; accepted date

ABSTRACT

ATCA H I and radio continuum observations of the peculiar southern galaxy IC 2554 and its surroundings reveal typical signatures of an interacting galaxy group. We detected a large H I cloud between IC 2554 and the elliptical galaxy NGC 3136B. The gas dynamics in IC 2554 itself, which is sometimes described as a colliding pair, are surprisingly regular, whereas NGC 3136B was not detected. The H I cloud, which emerges from IC 2554 as a large arc-shaped plume, has a size of ~ 30 kpc, larger than that of IC 2554. The total H I mass of the IC 2554 system is $\sim 2 \times 10^9 M_{\odot}$, a third of which resides in the H I cloud. It is possible that tidal interaction between IC 2554 and NGC 3136B caused this spectacular H I cloud, but the possibility of IC 2554 being a merger remnant is also discussed. We also detected H I gas in the nearby galaxies ESO 092-G009 and RKK 1959 as well as an associated H I cloud, ATCA J1006–6710. Together they have an H I mass of $\sim 4.6 \times 10^8 M_{\odot}$. Another new H I source, ATCA J1007–6659, with an H I mass of only $\sim 2.2 \times 10^7 M_{\odot}$ was detected roughly between IC 2554 and ESO 092-G009 and corresponds to a face-on low surface brightness dwarf galaxy. Star formation is evident only in the galaxy IC 2554 with a rate of $\sim 4 M_{\odot} \text{ yr}^{-1}$.

Key words: galaxies: individual (IC 2554, NGC 3136B, ESO 092-G009, RKK 1959)
— galaxies: interactions

1 INTRODUCTION

IC 2554 is a southern galaxy with a peculiar optical appearance. It is also known as Se 72/1 (Sérsic 1974), ESO 092-IG012, and IRAS 10075–6647. Fig. 1 shows a deep optical image of IC 2554 (Laustsen, Madsen & West 1987) revealing many bright knots as well as a network of dust lanes intersecting the main body of the galaxy. The optical extent of IC 2554 is $3'.25$ (see Table 1). Its irregular and asymmetric appearance has prompted the division into multiple components, roughly aligned North-South. Lauberts et al. (1978) describe IC 2554 as a ‘fox-shaped’ system with a complex spiral pattern. They distinguish three components: two central condensations separated by $18''$ with optical velocities of 1230 and 1310 km s^{-1} and a detached arm or satellite to the North (1190 km s^{-1}). Corwin et al. (1985) describe IC 2554 as a colliding pair (IC 2554A and B, $0'.8$ apart) with plumes. Laustsen et al. (1987) describe IC 2554 as a very disturbed pair of galaxies with a large number of emission nebulae,

indicating high activity of star formation. Lauberts (1982) and Laustsen et al. (1987) note IC 2554 as possibly disturbed by the elliptical galaxy NGC 3136B (ESO 092-G013). But IC 2554 has also been classified as a peculiar barred spiral galaxy (de Vaucouleurs et al. 1991), where the northern spiral arm appears elongated. High-resolution H I observations (presented here) are needed to study the gas dynamics of this complex system and distinguish between the numerous scenarios.

Close to IC 2554 (see Fig. 2) are three known galaxies: the elliptical galaxy NGC 3136B (1780 km s^{-1}), the faint spiral ESO 092-G009 and the galaxy RKK 1959. For a summary of various optical properties of IC 2554 and the neighbouring galaxies see Table 1.

With a Galactic latitude of $b = -9^{\circ}$ both the optical extinction (0.884 mag , Schlegel et al. 1998) and the density of foreground stars are relatively high. Despite this, numerous optical studies have been carried out. The optical velocities recorded for various positions within IC 2554 range from 1190 to 1474 km s^{-1} (Lauberts et al. 1978, Lauberts 1982, de Vaucouleurs et al. 1991, Fouqué et al. 1992, Sanders et al. 1995). The value of 1850 km s^{-1} also recorded by Fouqué et al. (1992) appears discrepant. Both Reif (1982) and Bot-

* The Australia Telescope Compact Array is part of the Australia Telescope which is funded by the Commonwealth of Australia for operation as a National Facility managed by CSIRO.

Table 1. Optical properties of the galaxy IC 2554 and catalogued galaxies within a radius of $90'$. Except for RKK 1959 and ESO 092-G009, only galaxies with known velocities in the range $1000\text{--}2200\text{ km s}^{-1}$ are included.

Name	Projected Distance	$\alpha, \delta(\text{J2000})$ [^{h,m,s}] [[°] , ['] , ^{''}]	Opt. velocity [km s^{-1}]	Morph. Type	Optical diameter	b_t [mag]	PA [[°]]	i [[°]]
IC 2554	—	10:08:50.5 –67:01:47	$1251 \pm 18^{(1)}$	SB3	$195'' \times 74''$	13.1	175	64
NGC 3136B	8'2	10:10:13.1 –67:00:18	$1780 \pm 31^{(1)}$	E4	$98'' \times 81''$	13.8	30	69
RKK 1959	13'9	10:06:37.3 –67:06:49	—	?	$20'' \times 20''$	17.6	—	face-on
ESO 092-G009	16'5	10:06:02.1 –67:03:48	—	I	$81'' \times 13''$	16.3	107	90
ESO 092-G014	25'9	10:10:52.2 –66:38:51	$1876 \pm 35^{(2)}$	F	$87'' \times 51''$	14.2	116	85
NGC 3136	27'4	10:05:48.0 –67:22:41	$1713 \pm 30^{(1)}$	E3	$215'' \times 161''$	12.3	30	62
RKK 1920	30'1	10:04:13.5 –66:48:43	$2081 \pm 84^{(2)}$	L	$56'' \times 56''$	15.0	—	face-on
ESO 092-G003	57'0	09:59:28.3 –67:18:18	$1478 \pm 207^{(2)}$	S1	$101'' \times 34''$	14.9	96	83
RKK 2182	66'6	10:15:43.3 –67:55:27	$1923 \pm 100^{(3)}$	S1	$40'' \times 15''$	16.5	—	62
ESO 092-G021	79'4	10:21:05.6 –66:29:31	$2002 \pm 52^{(2)}$	L	$74'' \times 60''$	14.5	48	58

References: The galaxy position in $\alpha, \delta(\text{J2000})$, morphological type, optical diameter, and the blue magnitude, b_t , are taken from Kraan-Korteweg (2000). All position angles (PA) are from de Vaucouleurs et al. (1991), and inclination angles (i) are mean values obtained from the Lyon-Meudon Extragalactic Database (LEDA). The velocity references are as follows: ⁽¹⁾ de Vaucouleurs et al. (1991); ⁽²⁾ Kraan-Korteweg et al. (1995); ⁽³⁾ Fairall, Woudt & Kraan-Korteweg (1998).

Tonry et al. (2001) derive distance moduli of 31.95 and 31.64 for NGC 3136 and NGC 3136B, respectively.

tinelli et al. (1990) measured an H I systemic velocity of $\sim 1378\text{ km s}^{-1}$ and an H I flux density of $\sim 30\text{ Jy km s}^{-1}$ for IC 2554 (see also Huchtmeier & Richter 1989). Aalto et al. (1995) obtained ^{12}CO and ^{13}CO measurements of IC 2554 and derive a ratio of $R_{1-0} = ^{12}\text{CO}(1-0)/^{13}\text{CO}(1-0) = 13 \pm 2$, which is at the high end for normal galaxies ($R_{1-0} \simeq 5\text{--}15$) but below the ratio of $R_{1-0} \simeq 20\text{--}50$ found for mergers (see Taniguchi et al. 1999).

Assuming $H_0 = 75\text{ km s}^{-1}\text{ Mpc}^{-1}$, we adopt a distance of $D = 16\text{ Mpc}$ for IC 2554 and associated galaxies ($1' = 4.7\text{ kpc}$). Throughout the paper, the quoted velocities are in the heliocentric velocity frame.

In the following we describe the observations and data reduction (Section 2), the H I results (Section 3), and the radio continuum results (Section 4). The discussion of the galaxies is presented in Section 5, followed by a comparison of various interaction and merger scenarios in Section 6. The conclusions are given in Sections 7.

2 OBSERVATIONS & DATA REDUCTION

IC 2554 has been observed with the Australia Telescope Compact Array (ATCA) from January 1997 through to March 1998. H I line and 13-cm radio continuum data have been obtained simultaneously using three 12-hour observations with the 750D, 1.5A, and 6B arrays, plus several shorter observations with the 375 array. The galaxy was also observed in the radio continuum at 6 and 3-cm for a total of 9 hours using the 1.5D array. For details of the observations see Table 2.

All data were calibrated with the *MIRIAD* software package, unless indicated otherwise, using standard procedures. The 20-cm data was split into a radio continuum and an H I line dataset using a first-order linear fit to the line-free channels. The H I channel maps (Figs. 3–5) were made using ‘natural’ weighting of the data in the velocity range from $1150\text{ to }2040\text{ km s}^{-1}$ (in steps of 10 km s^{-1}). The resulting synthesised beam is $29'.5 \times 28'.3$, and the measured r.m.s. is

$\sim 0.75\text{ mJy beam}^{-1}$. All data are corrected for primary-beam attenuation. The H I moment maps (Figs. 6–10) were produced with the *AIPS* task *MOMNT* using a spatial smoothing over 3 pixels and a flux cutoff of 3σ ($2.25\text{ mJy beam}^{-1}$).

All radio continuum maps were made using ‘natural’ weighting, resulting in synthesised beams of $18'.3 \times 18'.0$ (20-cm) and $9'.4 \times 9'.2$ (13-cm). The 6 and 3-cm radio observations were made at a slightly different pointing of $\alpha, \delta(\text{J2000}) = 10^{\text{h}} 08^{\text{m}} 55^{\text{s}}, -67^{\circ} 02' 00''$. The synthesised beams are $4'.2 \times 3'.6$ (6-cm) and $3'.4 \times 2'.9$ (3-cm). Edge channels attenuated by more than 50% were removed during calibration, leaving a bandwidth of 100 MHz at each frequency.

The measured r.m.s. noise is $0.068\text{ mJy beam}^{-1}$ (6-cm) and $0.053\text{ mJy beam}^{-1}$ (3-cm), compared to the theoretical noise of $0.054\text{ mJy beam}^{-1}$.

3 H I RESULTS

Fig. 6 shows the H I distribution of IC 2554 and its surroundings. We detect five distinct H I sources. Of these, IC 2554 together with an enormous H I extension to the East is the most remarkable source. Towards the SW, and close to the edge of the ATCA primary beam, a compact group of three H I sources is seen: the edge-on spiral galaxy ESO 092-G009, the galaxy RKK 1959 (Kraan-Korteweg 2000) and a new H I source, which is referred to here (by position) as ATCA J1006–6710. The fifth H I source, which lies roughly between IC 2554 and ESO 092-G009, is also new and in the following referred to as ATCA J1007–6659.

Because of their large angular separations and velocity differences, separate H I channel maps are presented for IC 2554 and its H I extension (Fig. 3), the compact group near ESO 092-G009 (Fig. 4) and ATCA J1007–6659 (Fig. 5).

All identified H I sources will be described separately in the following sections. A summary of the basic H I properties is given in Table 3. To calculate the H I mass we adopt a distance of $D = 16\text{ Mpc}$ for all H I sources in the neighbourhood of IC 2554, although we note that the systemic

Table 2. Observing parameters.

ATCA configurations	375, 750D, 1.5A, 6B (20 and 13-cm) 1.5D (6 and 3-cm)
Pointing position	10 ^h 09 ^m 00 ^s , -67° 02′ 00″
Primary calibrators	PKS 1934-638 or 0823-500
Secondary calibrators	PKS 0823-500, 1057-797 or 1036-097
H I data:	
Centre frequency	1413 MHz
Total bandwidth	8 MHz
No. of channels	512
Synthesised beam	29′.5 × 28′.3
r.m.s. noise	~0.75 mJy beam ⁻¹
Radio continuum data:	
Centre frequencies	2368/2496, 4800, 8640 MHz
Total bandwidth	128 MHz
No. of channels	32

velocities, v_{sys} , differ by several hundred km s^{-1} (see Table 1 & 3). It is not clear if these velocity differences are due to internal group dynamics or reflect the actual distances between the individual galaxies. In the latter case, IC 2554 and ESO 092-G009 would lie in the foreground, followed by RKK 1959 and ATCA J1006-6710, then NGC 3136B, and most distant ATCA J1007-6659. Tonry et al. (2001) derive a distance modulus of 31.64 for NGC 3136B, which corresponds to a distance 21.3 Mpc. Unfortunately, no independent distance estimate exists for IC 2554.

3.1 The Peculiar Galaxy IC 2554

The ATCA H I observations reveal a large amount of gas within the disk of the galaxy IC 2554 as well as an extended H I cloud to the East (Fig. 7). This broad H I tail or plume extends from the northern end of the disk to the North-East and then bends over nearly 180° counter-clockwise towards the South-East. The outer debris of the H I cloud appear to end just short of the elliptical galaxy NGC 3136B, which was not detected. The H I plume, which is substantially larger than IC 2554, has a projected length of at least $\sim 6'$ or 30 kpc in East-West direction. The surrounding H I debris possibly suggest an even larger extent at lower column densities.

Judging from the H I distribution alone, the plume resembles that of a companion galaxy centred on α , $\delta(\text{J2000}) = 10^{\text{h}} 09^{\text{m}} 5$, $-67^{\circ} 00'$, but no optical counterpart has been identified. The H I velocity field of the plume has no resemblance to that of a galaxy and is more likely due to a planar structure with relatively high velocity dispersion ($\sim 35 \text{ km s}^{-1}$, see Fig. 7d), indicating rather turbulent motions (see also Kregel & Sancisi 2001).

The IC 2554 system covers a velocity range from about 1240 to 1550 km s^{-1} (see Fig. 3) and contains a total H I mass of $\sim 2 \times 10^9 M_{\odot}$. The H I mass of the galaxy IC 2554 alone, which covers the entire velocity range, is $\sim 1.2 \times 10^9 M_{\odot}$. The H I plume, which covers the lower velocity range only (1240-1430 km s^{-1}), contains a slightly lower H I mass of $\sim 0.6 \times 10^9 M_{\odot}$, although the separation between plume and galaxy is not well defined.

A detailed look at the H I velocity field of IC 2554 (see Fig. 8) reveals a rather regularly rotating, nearly edge-on galaxy. The H I gas in the disk appears to follow the optical S-shape, which can be described as a bar (length $\sim 45''$, PA

$= 30^{\circ}$) and two emerging spiral arms. A signature of the bar is that the major and minor axes in that region of the disk are not perpendicular to each other. Towards the northern end of the disk the gas kinematics change drastically as one component still seems to follow the optically extended arm towards the North-West and another component traces the beginning of the H I plume in the opposite direction, towards the North-East.

The slight central depression in the H I distribution of IC 2554 is not unusual for spiral galaxies (e.g. M51, Rots et al. 1990). However, this does not mean there is a lack of neutral gas, as the central area contains a substantial amount of molecular gas (see Section 5.3). No H I absorption is visible in the channel maps.

3.1.1 Comparison with other H I measurements

Reif (1982) measured an H I systemic velocity of $1378 \pm 24 \text{ km s}^{-1}$, a velocity width of 400 km s^{-1} , and a total H I flux density of $29.3 \pm 3.5 \text{ Jy km s}^{-1}$ for IC 2554 (see also de Vaucouleurs et al. 1991, Huchtmeier & Richter 1989). Bottinelli et al. (1990) obtained very similar values, namely a 20% velocity line width of $393 \pm 12 \text{ km s}^{-1}$ and a total H I flux density of 30 Jy km s^{-1} . Both measurements were obtained with the Parkes 64-m telescope.

We measure a systemic velocity of $\sim 1380 \text{ km s}^{-1}$ and a velocity line width of $\sim 310 \text{ km s}^{-1}$ for IC 2554. Whereas the systemic velocity agrees with that measured by Reif (1982) and Bottinelli et al. (1990), the velocity line width strongly disagrees. This inconsistency can be resolved as both single-dish measurements also include some H I emission from the surrounding galaxies at slightly higher velocities. The H I flux densities given by Reif (1982) and Bottinelli et al. (1990) agree well with our measurement of $29.6 \text{ Jy km s}^{-1}$.

IC 2554 is clearly detected in the H I Parkes All-Sky Survey (HIPASS; see Staveley-Smith et al. 1996; Barnes et al. 2001). The HIPASS spectrum at the position of IC 2554 (Fig. 11) reveals H I emission in the velocity range from ~ 1220 to 1560 km s^{-1} , mostly associated with the IC 2554 system, and fainter emission from ~ 1560 to 2020 km s^{-1} , which can be attributed to the surrounding H I sources (see Fig. 3). A point source fit to IC 2554 gives an H I flux density of $\sim 21 \text{ Jy km s}^{-1}$, 50% and 20% velocity line widths of 240 km s^{-1} and 290 km s^{-1} , respectively, and a systemic ve-

Table 3. H I properties of the galaxy IC 2554 and surrounding H I sources.

Name	F_{HI} [Jy km s ⁻¹]	M_{HI}^* [10 ⁷ M _⊙]	α, δ (J2000) [^{h,m,s}] [^{°, ', ''}]		velocity range [km s ⁻¹]	v_{HI} [km s ⁻¹]
IC 2554	29.6	178.5	—	—	1240 – 1550	
– main body	19.3	116.4	10:08:50	–67:01:52	1240 – 1550	1380
– tidal cloud	10.3	62.1	10:09:30	–67:00:00	1240 – 1430	1310
ESO 092-G009	3.8	22.9	10:06:02	–67:03:45	1380 – 1520	1450
RKK 1959	2.8	16.9	10:06:36	–67:06:48	1570 – 1650	1610
ATCA J1006–6710	1.1	6.6	10:06:20	–67:09:14	1710 – 1730	1720
ATCA J1007–6659	0.4	2.2	10:07:29	–66:58:50	1970 – 2000	1985

*The H I mass was calculated using $M_{\text{HI}} = 2.356 \cdot 10^5 \cdot D^2 \cdot F_{\text{HI}}$ where F_{HI} is the H I flux density in Jy km s⁻¹. We adopt a distance of $D = 16$ Mpc for IC 2554 and the surrounding H I sources.

locity around 1395 km s⁻¹. We measure a flux density of ~ 9 Jy km s⁻¹ for the ESO 092-G009 / RKK 1959 group (1380 to 1800 km s⁻¹) and ~ 3 Jy km s⁻¹ for ATCA J1007–6659 (1800 to 2020 km s⁻¹). These flux densities are rather uncertain and depend strongly on the baseline subtraction and the integrated area.

3.2 ESO 092-G009 and RKK 1959

In the following we present the results for the compact group of three H I sources: the edge-on spiral galaxy ESO 092-G009, the galaxy RKK 1959 and the H I cloud ATCA J1006–6710. The H I channel maps are shown in Fig. 4, the H I moments in Fig. 9, and the H I spectra are displayed in Fig. 12. (Note that this galaxy group is located close to the edge of the ATCA primary beam, resulting in some uncertainty of the H I flux density estimates.)

ESO 092-G009 (RKK 1947) is a late-type spiral galaxy with no previously recorded velocity. Using the ATCA, we detected the galaxy in H I at a systemic velocity of 1450 km s⁻¹, which makes it a companion to IC 2554. The H I distribution of ESO 092-G009 (Fig. 9) resembles an edge-on disk with several faint extensions. The H I extent of ESO 092-G009 is about $3' \times 1'$, slightly larger than its optical size. We measure an H I mass of only 2.3×10^8 M_⊙. The H I velocity field of ESO 092-G009 is fairly regular, covering a velocity range from 1380 to 1520 km s⁻¹, and the H I velocity dispersion is typical for an edge-on galaxy.

RKK 1959 is a very faint, nearly face-on galaxy close to the Galactic Plane ($b = -9.2$, $A_B = 1.0$ mag) with an optical size of $\sim 20''$ (see Kraan-Korteweg 2000). Its projected distance from ESO 092-G009 is 4.6 or 21 kpc, if both galaxies are at a distance of 16 Mpc. The H I emission covers a velocity range from ~ 1570 to 1650 km s⁻¹ (see Fig. 5); the galaxy position angle is about $PA = 160^\circ$. There is an additional H I component around 1720 km s⁻¹ near the position of RKK 1959, which is likely to be part of the H I source ATCA J1006–6710. The H I velocity field and dispersion of RKK 1959 (Fig. 9) are strongly affected by this feature, which is discussed below. We measure an H I mass of 1.7×10^8 M_⊙ for RKK 1959, which is slightly lower than that of ESO 092-G009.

The new H I source, ATCA J1006–6710, lies North of RKK 1959 and ESO 092-G009 at projected distances of 2.9 and 5.7 , respectively. The channel maps best show the extended, but clumpy nature of the H I gas which covers a

very narrow velocity range of ~ 1710 to 1730 km s⁻¹. The northern most H I clumps in ATCA J1006–6710 overlap in position with the receding part of RKK 1959. Numerous H I clouds within the group (see Fig. 9), particularly between RKK 1959 and ATCA J1006–6710, suggest some tidal interaction between the group members. The clumpy nature of the gas in ATCA J1006–6710 as well as the velocity structure suggest it is a tidal H I cloud ($M_{\text{HI}} = 6.6 \times 10^7$ M_⊙) associated with the galaxy RKK 1959. Due to the high density of foreground stars it was not possible to identify an optical counterpart, although there appears to be a very faint (background) galaxy at α, δ (J2000) = $10^{\text{h}} 06^{\text{m}} 11^{\text{s}}$, $-67^\circ 10' 00''$, offset from the centre position but still within the irregular H I envelope of ATCA J1006–6710.

The galaxies ESO 092-G009 and RKK 1959 as well as a third source, ATCA J1006–6710, comprise a compact group with a total H I flux density of 7.7 Jy km s⁻¹ and a corresponding H I mass of $\sim 4.6 \times 10^8$ M_⊙. Are the members of this group interacting with each other? The H I distribution of ESO 092-G009 shows some irregular extensions indicating that the outer portions of the disk may have been disturbed. RKK 1959 also appears disturbed and ATCA J1006–6710 is most likely an associated tidal H I cloud. The systemic velocities of ESO 092-G009 and RKK 1959 differ by about 160 km s⁻¹, which could indicate quite a large separation. The best indicator for tidal interaction in this group is possibly the amount of H I cloudlets or debris between the galaxies.

3.3 The galaxy ATCA J1007–6659

The other new H I source, ATCA J1007–6659, lies roughly between IC 2554 and ESO 092-G009 at projected distances of 8.5 and 9.8 , respectively. It is barely resolved in H I and covers a narrow velocity range (~ 1970 to 2000 km s⁻¹). A very faint optical counterpart is visible in the second generation Digitised Sky Survey (DSSII) as well as in the blue UK Schmidt plates scanned with SuperCOSMOS (see Fig. 10). It appears to be an irregular, nearly face-on low-surface brightness galaxy with an optical diameter of $\sim 20''$. ATCA J1007–6659 contains an H I mass of 2.2×10^7 M_⊙. We estimate a systemic velocity of ~ 1985 km s⁻¹, which is substantially higher than that of IC 2554 ($v_{\text{HI}} = 1380$ km s⁻¹) and indicates that ATCA J1007–6659 probably lies at a larger distance.

4 RADIO CONTINUUM RESULTS

Of the HI sources described here, only the peculiar galaxy IC 2554 was detected in the radio continuum. Figs. 13–15 show the maps at all four frequencies. We measure the following flux densities: 101 mJy (1413 MHz), 65 mJy (2496 MHz), 29.5 mJy (4800 MHz), and 10.8 mJy (8640 MHz). IC 2554 is also known as the radio continuum source PMN J1008–6701 for which Wright et al. (1994) measured a flux density of 37 ± 7 mJy at 4.85 GHz.

The radio continuum emission of IC 2554 is extended at all four frequencies. It is dominated by a central source with a maximum at $10^{\text{h}} 08^{\text{m}} 50^{\text{s}}.2$, $-67^{\circ} 01' 54''$, coinciding with the center of the barred region, but a few arcseconds South-West of the previously catalogued galaxy center (see Table 1). The sensitive 13-cm map (Fig. 14) shows most clearly the extent across the central bar of IC 2554 and emission at the beginning of the spiral arms, possibly following the dust lanes (particularly in the North).

4.1 Star Formation in IC 2554

For an individual star-forming galaxy, the star formation rate (SFR) is directly proportional to its radio luminosity, L_{ν} , (Condon 1992, Haarsma et al. 2000). The radio continuum emission of IC 2554 arises from the central disk and two emerging spiral arms. The latter are only visible in the 20 and 13-cm radio continuum emission. The total SFR, as estimated from those maps, is $\sim 4 M_{\odot} \text{ yr}^{-1}$ (see Table 4 for the results at all frequencies). The 6-cm radio continuum emission was detected only across the central bar and the 3-cm emission comes mostly from the nucleus.

The far-infrared luminosity, L_{FIR} , of IC 2554, as determined from the IRAS 60 and $100 \mu\text{m}$ flux densities, is $8.3 \times 10^9 L_{\odot}$. This value is low compared to $L_{\text{FIR}} \gtrsim 10^{11} L_{\odot}$ for luminous starburst mergers. Following Hunter et al. (1986) we derive $\text{SFR} = 2.1 M_{\odot} \text{ yr}^{-1}$, about half the value determined from the 13 and 20-cm radio continuum observations. IC 2554 is clearly resolved at 12 and $25 \mu\text{m}$, and marginally resolved at $100 \mu\text{m}$ (Sanders et al. 1995).

The nuclear H_2 mass, M_{H_2} , of IC 2554 is $\sim 0.4 \times 10^9 M_{\odot}$ which is derived using the standard conversion factor of the CO line intensity (Aalto et al. 1995) to the molecular hydrogen column density.

We derive a star formation efficiency (SFE) of $L_{\text{FIR}}/M_{\text{H}_2} \lesssim 21 L_{\odot}/M_{\odot}$, well above the threshold of $4 L_{\odot}/M_{\odot}$ for star-forming galaxies. Note that L_{FIR} comes from the whole galaxy disk whereas M_{H_2} was only measured in the galaxy centre; our value of $L_{\text{FIR}}/M_{\text{H}_2}$ is therefore an overestimate. Loiseau & Combes (1993) find nuclear and extranuclear CO(1–0) emission in IC 2554.

5 DISCUSSION

The peculiar optical appearance of IC 2554 has prompted numerous suggestions as to its nature (see Section 1). Is IC 2554 interacting with a neighbour galaxy or is it a merging galaxy pair? The shape of the extended HI distribution and the gas kinematics as well as the peculiar optical appearance of IC 2554 should give us clues as to its history.

Toomre & Toomre (1972) showed that the double tailed

Table 4. Radio continuum flux densities, luminosities and star formation rates for IC 2554.

ν (GHz)	F_{ν} [mJy]	L_{ν} [$10^{20} \text{ W Hz}^{-1}$]	SFR [$M_{\odot} \text{ yr}^{-1}$]
1.413	101	30.94	3.7
2.496	65	19.91	3.6
4.800	29.5	9.04	2.5
8.640	10.8	3.31	1.4

morphology of many galaxy systems is the signature of merging pairs of disk galaxies (see also Barnes 1988). One tail arises from each progenitor galaxy, on roughly opposing sides of the remnant. This is particularly true for interacting pairs of comparable mass (Barnes & Hernquist 1992, 1996). ‘The Antennae’ (NGC 4038/39) is a prominent example of this kind of merger (Gordon et al. 2001, Hibbard et al. 2001). In contrast to NGC 4038/39, the peculiar galaxy IC 2554 shows only a single tail or HI plume, mild star-formation, and a regularly rotating disk. The lack of a second surviving arm suggests some difference in the mass, structure, or gas content of the progenitor galaxies. For example, it is possible that only one of the progenitors was gas-rich, producing a single gaseous tail. *But is IC 2554 a merger remnant?* The HI velocity field appears very regular, in contrast to what we would expect from the violent merging of two galaxy disks. The latter is only true for a merger of comparable-mass galaxies, which eliminates many of the initial characteristics of both progenitors in the formation of a new galaxy (Bendo & Barnes 2000). Mergers between galaxies of significantly different masses are less violent, and for sufficiently large mass ratios, the more massive galaxy may survive essentially unscathed. The mild star-formation, regular disk kinematics and one-sided HI plume suggest IC 2554 may be the remnant of a merger between highly unequal-mass galaxies.

In the following we first explore the possibility of tidal interactions between IC 2554 and (1) the elliptical galaxy NGC 3136B to the East (Section 6.1) and (2) the spiral galaxy ESO 092-G009 to the South-West (Section 6.2). In these scenarios the northern elongated feature in optical images of IC 2554 (Fig. 1) is interpreted as a tidally distorted spiral arm. After comparison with similar systems in the literature (Section 6.3) we also discuss the possibility of a merger event. In that case the northern elongated feature and the central region of IC 2554 represent the remnants of the two merging galaxies. The existence of a rather normally rotating disk in IC 2554, as observed in HI, is most remarkable.

5.1 The elliptical galaxy NGC 3136B

The elliptical galaxy NGC 3136B is, with a projected distance of $8'.2$, possibly the closest neighbour to IC 2554 (see Table 1) and therefore a potential interaction partner. Although its distance modulus and systemic velocity (1780 km s^{-1}) suggest a much larger distance than IC 2554. A tidal interaction is only possible if the two galaxies are relatively close, in which case substantial peculiar motions are present in the group. In the following we assume that

NGC 3136B is at the same distance as IC 2554 ($D = 16$ Mpc), as noted in Section 3.

No evidence for any disturbance has been found in the optical images of NGC 3136B. It was not detected in H I and we derive an upper limit to the H I mass of $10^7 M_{\odot}$, assuming a velocity width of 100 km s^{-1} . McElroy (1995) measure an optical velocity dispersion of $\sigma_v = 165 \text{ km s}^{-1}$ for NGC 3136B which gives a total dynamical mass of $2.4 \times 10^{10} M_{\odot}$ using $M_{\text{tot}} = 2.31 \times 10^5 R_c \sigma_v^2$ with a core radius of $R_c = 3.8 \text{ kpc}$ (see Table 1). The extinction-corrected blue magnitude for NGC 3136B ($b_{\text{tc}} \sim 13 \text{ mag}$) corresponds to a blue luminosity of $L_B \sim 1.4 \times 10^9 L_{\odot}$. This is consistent with the $L_B \propto \sigma_v^4$ relation (Faber & Jackson 1976). The resulting mass-to-light ratio is $M/L_B = 17$.

The gas-rich spiral IC 2554 and the gas-poor elliptical NGC 3136B have quite similar total masses, 2.4 and $3.2 \times 10^{10} M_{\odot}$, respectively, and would make a spectacular interaction pair if they were close. Preliminary results from numerical simulations by Horellou (2002, priv. comm.) suggest that the H I plume and the large difference in systemic velocities ($\Delta v \sim 400 \text{ km s}^{-1}$) could be the result of a parabolic encounter of the two galaxies.

We note that to the East of NGC 3136B, and very close to the bright star HD 309888, lies another small, uncatalogued galaxy at $\alpha, \delta(\text{J2000}) = 10^{\text{h}} 10^{\text{m}} 43^{\text{s}}, -67^{\circ} 01' 00''$.

5.2 The spiral galaxy ESO 092-G009

The other neighbour to IC 2554 is the highly-inclined spiral galaxy ESO 092-G009, at a projected distance of $16'.5$. The systemic velocities of both galaxies differ by only 80 km s^{-1} (see Table 3), suggesting a separation of $\gtrsim 77 \text{ kpc}$.

Although the H I velocity field of ESO 092-G009 is regular, the galaxy shows some H I extensions which could be due to tidal interactions. The closest neighbour to ESO 092-G009 is the galaxy RKK 1959, which is also accompanied by a tidal H I cloud. There is evidence for tidal interactions within this group (see Fig. 5), so it is difficult to attribute any distortions to the relatively distant galaxy IC 2554.

The total dynamical mass of ESO 092-G009 is $2.6 \times 10^9 M_{\odot}$, substantially less than that of NGC 3136B ($2.4 \times 10^{10} M_{\odot}$) or IC 2554 ($3.2 \times 10^{10} M_{\odot}$). RKK 1959 has a total mass similar to that of ESO 092-G009 if we assume an inclination of 20° .

In an interaction involving two galaxies of different sizes/masses (e.g. IC 2554 and ESO 092-G009), the smaller, less-massive galaxy should be the most disrupted, since it exerts smaller tidal forces on material in its companion, and it has less ability to resist tidal disruption of its own material. So, here we do have a close interaction partner, in fact a group of galaxies, but together they only comprise a quarter of the total mass of IC 2554. Although this group might have played a role in the interaction scenario, it is, most likely, not able to produce the H I plume observed in IC 2554.

5.3 Comparison with similar systems

The ‘H I Rogues Gallery’ (Hibbard et al. 2001) provides a compilation of H I maps of peculiar galaxies and is very useful for the comparison and understanding of e.g. interacting

and merging galaxies. We find that the extended H I distributions of the following systems have some similarity to that of IC 2554: M 51 (Rots et al. 1990), NGC 3310 (Kregel & Sancisi 2001), NGC 2146 (Taramopoulos et al. 2001), NGC 3227 (Mundell et al. 1995) and NGC 520 (Stanford & Balcells 1991, Hibbard & van Gorkom 1996).

H I observations of the galaxy M 51 (NGC 5194) by Rots et al. (1990) reveal a spiral structure in the inner regions and faint H I extensions at larger radii (up to 21 kpc) with a very complicated velocity structure. In addition, they find that from the South a broad H I tail (similar to that of IC 2554) curves towards the North and East, over a projected length of 90 kpc . No strong H I emission is associated with the companion NGC 5195. Detailed numerical simulations of NGC 5194/5 by Salo & Laurikainen (2000) reproduce many of the observed features; the best result is achieved using a multiple-encounter model with a recent passage of the companion. Salo & Laurikainen note that the pre-existing spiral arms are washed out by the tidally triggered spiral arms.

H I observations of the peculiar spiral galaxy NGC 2146 by Taramopoulos et al. (2001) reveal two elongated streams of gas extending up to six Holmberg radii. The authors propose that these streams were produced by tidal interactions between NGC 2146 and a low-surface brightness companion which was destroyed in the encounter and remain undetected at optical wavelengths. The H I kinematics in the inner part of NGC 2146 are quite distorted although some resemblance to a rotating disk remains.

H I observations of the spiral galaxy NGC 3227 by Mundell et al. (1995) reveal H I plumes extending $\sim 70 \text{ kpc}$ North and $\sim 31 \text{ kpc}$ South. These may be a consequence of interaction with the elliptical companion galaxy NGC 3226, which is located at the base of the northern plume, but was not detected in H I. Again, the disk of NGC 3227 is, despite the proposed encounter, in relatively undisturbed solid-body rotation.

H I observations of the isolated spiral galaxy NGC 3310 (Arp 217) by Kregel & Sancisi (2001) reveal a rotating disk and two H I tails resembling the tidal tails seen in gravitationally interacting systems or mergers. The large velocity dispersion of the inner parts of the galaxy suggests a highly perturbed disk. According to Kregel & Sancisi all evidence points to a recent merger event, possibly of two galaxies with small but comparable masses, at least one of which is gas-rich. They note the remarkable existence of a disk after such an apparently ‘‘major’’ merger event and propose that the unsettled disk could be either a newly formed disk with spiral arms and on-going star formation or the disturbed disk of one of the progenitors which has survived the merger and is now undergoing new star formation.

If the massive H I plume emerging from IC 2554 cannot be explained by tidal interactions of IC 2554 with the elliptical galaxy NGC 3136B, we need to consider the possibility that IC 2554 is a merger remnant. There are other examples in the literature (see above) which support such a scenario for IC 2554. An equal mass encounter would have destroyed the progenitor disks, but simulations by Barnes (2002) show that in the merger remnant a disk can be rebuilt. This would be accompanied by high star formation. Or alternately, a merger of two galaxies with large mass difference would leave the more massive galaxy nearly intact whereas the less massive galaxy gets destroyed. Elmegreen et

al. (1993) consider interactions between galaxies with nearly equal masses and with *extended gas disks* to explain the formation of cloud complexes seen in NGC2163/NGC 2207. They also find that large gas disks lead to an extended gas pool at the end of the tidal tail. This might also apply to IC 2554.

6 CONCLUSIONS

The peculiar galaxy IC 2554 and its surroundings were observed with the ATCA in both the H I emission line as well as the radio continuum. In addition to IC 2554 itself, which — contrary to its peculiar optical appearance — shows a surprisingly regular H I velocity field, we detected a large tidal H I plume East of IC 2554 as well as numerous neighbouring galaxies and H I clouds. Radio continuum emission was only detected in IC 2554, where it broadly follows the optical shape of the galaxy.

H I observations of IC 2554 reveal a very broad tail or H I plume with a projected length of at least 30 kpc. The extent, shape and mass of the plume, which shows a relatively high velocity dispersion, as well as the H I debris surrounding IC 2554 and the plume indicate that a major merger or interaction event has happened. This is supported by the peculiar optical appearance of the galaxy IC 2554. Optical knots seen throughout the body of the galaxy suggest on-going star formation, however star formation rates determined from the radio continuum emission are at $\sim 4 M_{\odot} \text{ yr}^{-1}$ not very high.

The edge-on spiral galaxy ESO 092-G009 is most likely the closest neighbour to IC 2554 with a separation of $\gtrsim 77$ kpc. Although the inner part of its velocity field appears regular, the outer H I layer of ESO 092-G009 is clearly disturbed. Some asymmetry is also seen in the optical appearance. The small galaxy RKK 1959, just South-East of ESO 092-G009 has an H I mass of $1.7 \times 10^8 M_{\odot}$ and a systemic velocity of $\sim 1610 \text{ km s}^{-1}$. It appears rather disturbed and is associated with the H I cloud ATCA J1006–6710. All three H I sources together build a compact group which appears to be mildly interacting with each other.

It is unlikely that the H I plume was created by tidal interactions of IC 2554 with ESO 092-G009 / RKK 1959, because of the large difference in total mass, which would have disrupted the latter, less-massive system.

We suggest that the H I plume is the result of a major merger or interaction between the gas-rich galaxy IC 2554 and a less massive companion galaxy. The fact that IC 2554 has a regularly rotating disk suggests that either the disk was not destroyed during the encounter or it was rebuilt through tidal forces. The gas-poor galaxy NGC 3136B would qualify as the interaction partner only if it was at a distance similar to IC 2554. In that case the large difference in redshifts needs to be explained by peculiar motions within the group. If NGC 3136B is not the interaction partner, then IC 2554 must be the result of a major merger where either the unknown intruder was destroyed and the disk of IC 2554 perturbed or both progenitors merged to form a new disk. The latter scenario is explored by Barnes (2002) who finds that extended gaseous disks can settle well after the merger has happened leaving one or more tidal tails as the main signature of the merger event. The bar and extended star formation in IC 2554 are likely consequences of

such a merger event. The displacement of some stellar and gaseous tidal features can be explained naturally by the extended gas disks of galaxies; it also puts constraints on the merger geometry (Mihos 2001).

ACKNOWLEDGEMENTS

- We thank S. Laustsen, C. Madsen and R.M. West for their kind permission to reproduce the optical image of IC 2554. Credit: European Southern Observatory (ESO)
- We acknowledge use of Digitized Sky Survey (DSS) material (UKST/ROE/AAO/STScI) and the SuperCOSMOS Sky Surveys (SSS).
- This research has made use of the NASA/IPAC Extragalactic Database (NED) which is operated by the Jet Propulsion Laboratory, California Institute of Technology, under contract with the National Aeronautics and Space Administration.
- HIPASS Data were provided by the ATNF under the auspices of the Multibeam Survey Working Group.

REFERENCES

- Aalto, S., Booth, R.S., Black, J.H., Johansson, L.E.B. 1995, *A&A* 300, 369
- Barnes, J.E. 1988, *ApJ* 331, 699
- Barnes, J.E. 2002, *MNRAS* 333, 481
- Barnes, J.E., Hernquist, L. 1992, *Nature*, 360, 715
- Barnes, J.E., Hernquist, L. 1996, *ApJ*, 471, 115
- Barnes, D.G., et al. 2001, *MNRAS* 322, 486
- Bendo, G.J., Barnes, J.E. 2000, *MNRAS* 316, 315
- Bottinelli, L., Gouguenheim, L., Fouqué, P., Paturel, G. 1990, *A&AS*, 82, 391
- Condon, J.J. 1992, *ARA&A*, 30, 575
- Corwin, H.G. Jr., de Vaucouleurs, A., de Vaucouleurs, G. 1985, ‘Southern Galaxy Catalogue’, U. Texas, Austin
- de Vaucouleurs, G., de Vaucouleurs, A., Corwin, H.G. Jr., Buta, R.J., Paturel, G., Fouqué, P. 1991, ‘Third Reference Catalogue of Bright Galaxies’, New York: Springer Verlag [RC3]
- Elmegreen, B.G., Kaufman, M., Thomasson, M. 1993, *ApJ*, 412, 90
- Faber, S.M., Jackson, R.E. 1976, *ApJ* 204, 668
- Fairall, A.P., Woudt, P.A., Kraan-Korteweg, R.C. 1998, *A&AS*, 127, 463
- Fouqué, P., Durand, N., Bottinelli, L., Gouguenheim, L., Paturel, G. 1992, *Catalogue of Optical Radial Velocities*
- Gordon, S., Koribalski, B., Jones, K. 2001, *MNRAS*, 326, 578
- Haarsma, D.B., Partridge, R.N., Windhorst, R.A., Richards, E.A. 2000, *ApJ*, 544, 641
- Hibbard, J.E., van Gorkom, J.H. 1996, *AJ* 111, 655
- Hibbard, J.E., van der Hulst, J.M., Barnes, J.E., Rich, R.M. 2001, *AJ* 122, 2969
- Hibbard, J.E., van Gorkom, J.H., Rupen, M.P., Schiminovich, D. 2001, in ‘Gas & Galaxy Evolution’, ASP Conf. Series, Vol. 240, eds. J.E. Hibbard, M.P. Rupen and J.H. van Gorkom, p. 659
- Huchtmeier, W.K., Richter, O.-G. 1989, ‘A General Catalog of H I Observations of Galaxies’, Springer-Verlag, New York
- Hunter, D.A., Gillett, F.C., Gallagher, J.S., III, Rice, W.L., Low, F.J. 1986, *ApJ* 303, 171
- Kraan-Korteweg, R.C., Fairall, A.P., Balkowski, C. 1995, *A&A*, 297, 617
- Kraan-Korteweg, R.C. 2000, *A&AS*, 141, 123
- Kregel, M., Sancisi, R. 2001, *A&A* 376, 59

- Lauberts, A. 1982, 'The ESO/Uppsala Survey of the ESO(B) Atlas', Munich: European Southern Observatory
- Lauberts, A., Bergvall, N.A.S., Ekman, A.B.G., Westerlund, B.E. 1978, *A&AS*, 35, 55
- Laustsen, S., Madsen, C., West, R.M. 1987, 'Exploring the Southern Sky : A Pictorial Atlas from the European Southern Observatory (ESO)', Springer-Verlag
- Loiseau, N., Combes, F. 1993, *RMxA&A* 26, 123
- McElroy, D.B. 1995, *ApJS* 100, 105
- Mihos, J.C. 2001, *ApJ* 550, 94
- Mundell, C.G., Pedlar, A., Axon, D.J., Meaburn, J., Unger, S.W. 1995, *MNRAS* 277, 641
- Reif, K. 1982, PhD Thesis, University of Bonn
- Rots, A.H., Bosma, A., van der Hulst, J.M., Athanassoula, E., Crane, P.C. 1990, *AJ* 100, 387
- Salo, H., Laurikainen, E. 2000, *MNRAS* 319, 377
- Sanders, D.B., Egami, E., Lipari, S., Mirabel, I.F., Soifer, B.T. 1995, *AJ* 110, 1993
- Schlegel, D.J., Finkbeiner, D.P., Davis, M. 1998, *ApJ*, 500, 525
- Sérsic, J.L. 1974, *AP&SS*, 28, 365
- Stanford, S.A., Balcells, M. 1991, *ApJ* 370, 118
- Staveley-Smith, L., et al. 1996, *PASA* 13, 243
- Taramopoulos, A., Payne, H., Briggs, F.H. 2001, *A&A* 365, 360
- Taniguchi, Y., Ohya, Y., Sanders, D.B. 1999, *ApJ* 522, 214
- Tonry, J.L., Dressler, A., et al. 2001, *ApJ* 546, 681
- Toomre, A., Toomre, J. 1972, *ApJ*, 178, 623
- Wright, A.E., Griffith, M.R., Burke, B.F., Ekers, R.D. 1994, *ApJS*, 91, 111

Figure 1. Optical image of the peculiar galaxy IC 2554, reproduced from Plate 88 in Laustsen, Madsen & West (1987), with kind permission from the authors. The white cross indicates the peak of the radio continuum emission.

Figure 2. Optical image of the galaxy IC 2554 and its surroundings, obtained from the Digitised Sky Survey.

Figure 3. HI channel maps covering the area around the peculiar galaxy IC 2554, the tidal HI cloud and the elliptical galaxy NGC 3136B. The contours levels are $\pm 2.25, 4.5, 9.0,$ and $18.0 \text{ mJy beam}^{-1}$ ($3\sigma \times 2^n$ with $\sigma = 0.75 \text{ mJy beam}^{-1}$). The synthesised beam ($29''.5 \times 28''.3$) is displayed at the bottom left, and heliocentric velocities (in km s^{-1}) are displayed at the top left of each panel.

Figure 3. — continued.

Figure 3. — continued.

Figure 4. HI channel maps covering the area around ESO 092-G009, RKK 1959 and the HI cloud ATCA J1006-6710. The contours levels are $\pm 3.9, 7.8, 15.6,$ and $31.2 \text{ mJy beam}^{-1}$ ($3\sigma \times 2^n$ with $\sigma = 1.3 \text{ mJy beam}^{-1}$). The synthesised beam ($29''.5 \times 28''.3$) is displayed at the bottom left, and heliocentric velocities (in km s^{-1}) are displayed at the top left of each panel.

Figure 4. — continued.

Figure 4. — continued.

Figure 5. HI channel maps for the newly discovered galaxy ATCA J1007-6659, which lies roughly between IC 2554 and ESO 092-G009. The contour levels are $\pm 3.9, 5.5,$ and $7.8 \text{ mJy beam}^{-1}$ ($3\sigma \times 2^{n/2}$ with $\sigma = 1.3 \text{ mJy beam}^{-1}$). The synthesised beam ($29''.5 \times 28''.3$) is displayed at the bottom left, and heliocentric velocities (in km s^{-1}) are displayed at the top left of each panel.

Figure 6. HI intensity distribution of IC 2554 and the surrounding field. Clearly visible are the galaxy IC 2554 (left), ESO 092-G009, RKK 1959 and the two new objects (ATCA J1006–6710 and ATCA J1007–6659). The greyscale ranges from 0 to $1.75 \text{ Jy beam}^{-1} \text{ km s}^{-1}$. The contour levels are $-0.02, 0.02, 0.04, 0.08, 0.16, 0.32, 0.64,$ and $1.28 \text{ Jy beam}^{-1} \text{ km s}^{-1}$. The beam is indicated at the bottom left ($29''.5 \times 28''.3$).

Figure 7. HI moment maps of the peculiar galaxy IC 2554. **(a)** HI intensity distribution overlaid onto an optical image from the Digitised Sky Survey (DSS). The contour levels are $\pm 0.02, 0.04, 0.08, 0.16, 0.32, 0.64,$ and $1.28 \text{ Jy beam}^{-1} \text{ km s}^{-1}$. **(b)** HI intensity distribution; contour levels as in **(a)**. **(c)** Mean HI velocity field. The contour levels range from 1275 to 1525 km s^{-1} in steps of 25 km s^{-1} . **(d)** HI velocity dispersion. The contour levels are $5, 10, 20, 40,$ and 80 km s^{-1} . The beam is indicated at the bottom left of each image ($29''.5 \times 28''.3$).

Figure 8. Close-ups of the HI moment maps. **(left)** HI intensity distribution showing only IC 2554 overlaid onto the optical image (see Fig. 1). The contour levels are $\pm 0.02, 0.04, 0.08, 0.16, 0.32, 0.64,$ and $1.28 \text{ Jy beam}^{-1} \text{ km s}^{-1}$ (as in Fig. 7). **(right):** Mean HI velocity field. The contours levels are in steps of 25 km s^{-1} , increasing from 1275 to 1525 km s^{-1} . Regions with HI flux density below $0.04 \text{ Jy beam}^{-1} \text{ km s}^{-1}$ have been masked out. — The beam is indicated at the bottom left of each image.

Figure 9. HI moment maps showing in closeup ESO 092-G009, RKK 1959, and the newly-discovered object ATCA J1006–6710. **(a)** HI intensity distribution overlaid onto a 2nd-generation DSS optical image. The contour levels are $\pm 0.04, 0.08, 0.16, 0.32,$ and $0.64 \text{ Jy beam}^{-1} \text{ km s}^{-1}$. **(b)** HI intensity distribution, contours levels as in **(a)**; the greyscale ranges from 0 to $1.75 \text{ Jy beam}^{-1} \text{ km s}^{-1}$. **(c)** Mean HI velocity field. The contour levels range from 1400 to 1512.5 km s^{-1} in steps of 12.5 km s^{-1} (ESO 092-G009) and from 1575 to 1725 km s^{-1} in steps 25 km s^{-1} (others); the greyscale ranges from 1350 to 1850 km s^{-1} . **(d)** HI velocity dispersion. The contour levels are $5, 10, 20, 30, 40, 50, 60,$ and 70 km s^{-1} .

Figure 10. HI intensity distribution of the newly discovered galaxy ATCA J1007–6659 overlaid onto an optical image obtained from the blue UK Schmidt plates. The contour levels are $\pm 0.02, 0.04, 0.08, 0.12$ and $0.16 \text{ Jy beam}^{-1} \text{ km s}^{-1}$.

Figure 11. HIPASS spectrum at the position of the peculiar galaxy IC 2554. A zero-th order baseline was fitted to the spectrum outside the dashed lines; the HI emission was fitted inside the dotted lines (see Section 5.1).

Figure 12. HI spectra for IC 2554, ESO 092-G009, RKK 1959 and the newly-detected objects ATCA J1006–6710 and ATCA J1007–6659.

Figure 13. 20-cm radio continuum image of IC 2554 (contours), overlaid onto the optical image (see Fig. 1). The contour levels are $\pm 0.78, 1.10, 1.56, 2.2, 3.1, 4.4, 6.2, 8.8, 12.5, 17.6, 35.3,$ and 50 mJy beam^{-1} ($3\sigma \times 2^{n/2}$). The beam is displayed at the bottom left ($18''.3 \times 18''.0$).

Figure 14. 13-cm radio continuum image of IC 2554 (contours), overlaid onto the optical image (see Fig. 1). The contour levels are $\pm 0.2, 0.28, 0.4, 0.56, 0.8, 1.14, 1.6, 2.3, 3.2, 4.5, 6.4, 9.1, 12.8, 18.1 \text{ mJy beam}^{-1}$ ($3\sigma \times 2^{n/2}$). The beam is displayed at the bottom left ($9''.4 \times 9''.2$).

Figure 15. **(left)** 6-cm radio continuum image of IC 2554 (contours), overlaid onto the optical image (see Fig. 1). The contour levels are $\pm 0.20, 0.29, 0.41, 0.58, 0.82, 1.16, 1.64, 2.31, 3.27, 4.63,$ and $6.55 \text{ mJy beam}^{-1}$ ($3\sigma \times 2^{n/2}$). The beam is displayed at the bottom right ($4''.2 \times 3''.6$). — **(right)** 3-cm radio continuum image of IC 2554 (contours), overlaid onto the optical image (see Fig. 1). The contour levels are $\pm 0.16, 0.22, 0.32, 0.45, 0.63, 0.89, 1.26, 1.79, 2.53,$ and $3.57 \text{ mJy beam}^{-1}$ ($3\sigma \times 2^{n/2}$). The beam is displayed at the bottom right ($3''.4 \times 2''.9$).

This figure "eso92-g9.mom0.gif" is available in "gif" format from:

<http://arxiv.org/ps/astro-ph/0211391v1>

This figure "ic2554.mom0.all.gif" is available in "gif" format from:

<http://arxiv.org/ps/astro-ph/0211391v1>

This figure "ic2554.mom0.gif" is available in "gif" format from:

<http://arxiv.org/ps/astro-ph/0211391v1>

This figure "ic2554.mom0.mod.gif" is available in "gif" format from:

<http://arxiv.org/ps/astro-ph/0211391v1>

This figure "eso92-g9.mom1.gif" is available in "gif" format from:

<http://arxiv.org/ps/astro-ph/0211391v1>

This figure "ic2554.AIPSmom1.gif" is available in "gif" format from:

<http://arxiv.org/ps/astro-ph/0211391v1>

This figure "ic2554.HIchannel1.gif" is available in "gif" format from:

<http://arxiv.org/ps/astro-ph/0211391v1>

This figure "ic2554.HIother1.gif" is available in "gif" format from:

<http://arxiv.org/ps/astro-ph/0211391v1>

This figure "ic2554.mom1.gif" is available in "gif" format from:

<http://arxiv.org/ps/astro-ph/0211391v1>

This figure "eso92-g9.mom0_2.gif" is available in "gif" format from:

<http://arxiv.org/ps/astro-ph/0211391v1>

This figure "eso92-g9.mom2.gif" is available in "gif" format from:

<http://arxiv.org/ps/astro-ph/0211391v1>

This figure "ic2554.HIchannel2.gif" is available in "gif" format from:

<http://arxiv.org/ps/astro-ph/0211391v1>

This figure "ic2554.HIother2.gif" is available in "gif" format from:

<http://arxiv.org/ps/astro-ph/0211391v1>

This figure "ic2554.mom0_2.gif" is available in "gif" format from:

<http://arxiv.org/ps/astro-ph/0211391v1>

This figure "ic2554.mom2.gif" is available in "gif" format from:

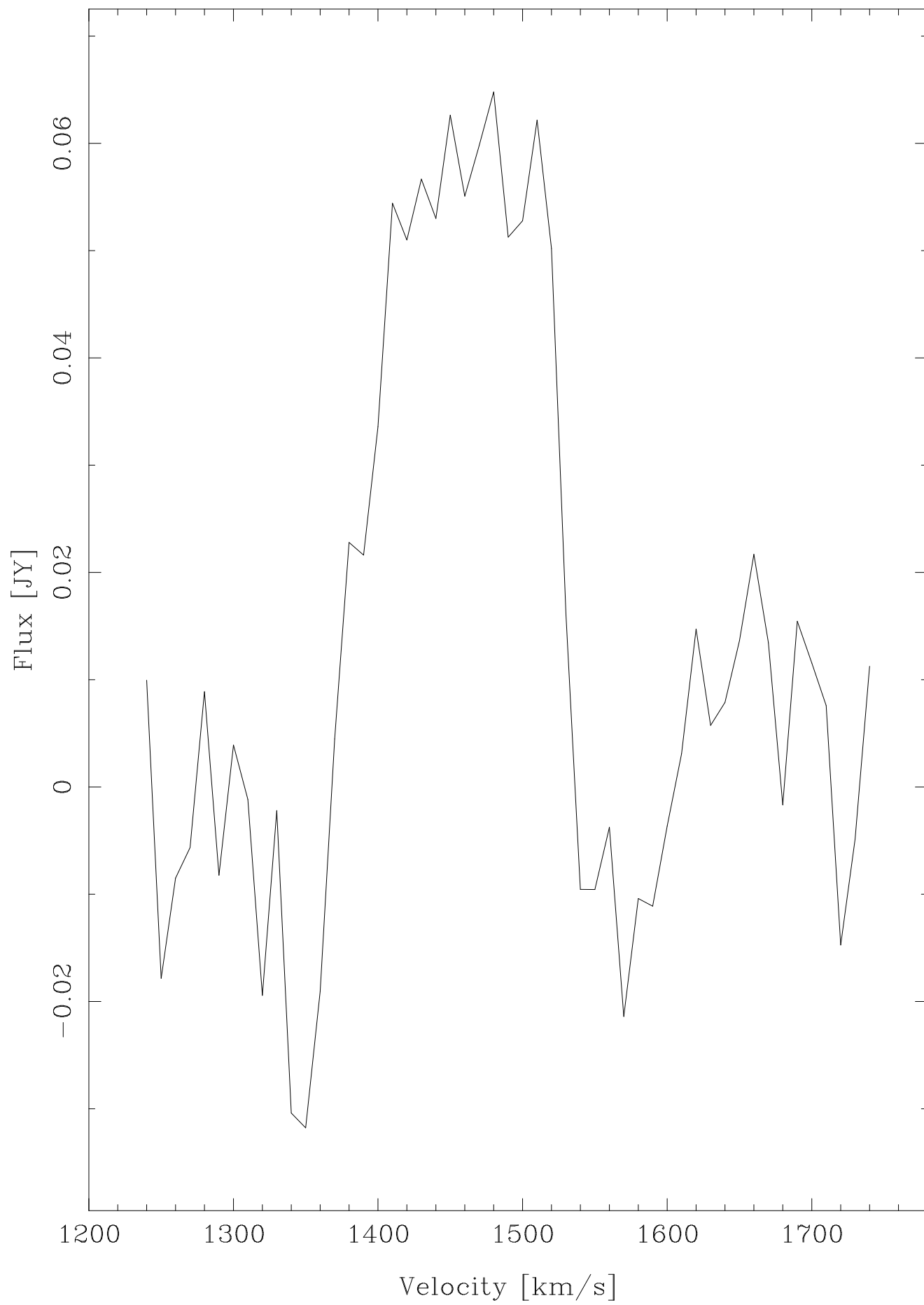
<http://arxiv.org/ps/astro-ph/0211391v1>

This figure "ic2554.HIchannel3.gif" is available in "gif" format from:

<http://arxiv.org/ps/astro-ph/0211391v1>

This figure "ic2554.HIother3.gif" is available in "gif" format from:

<http://arxiv.org/ps/astro-ph/0211391v1>

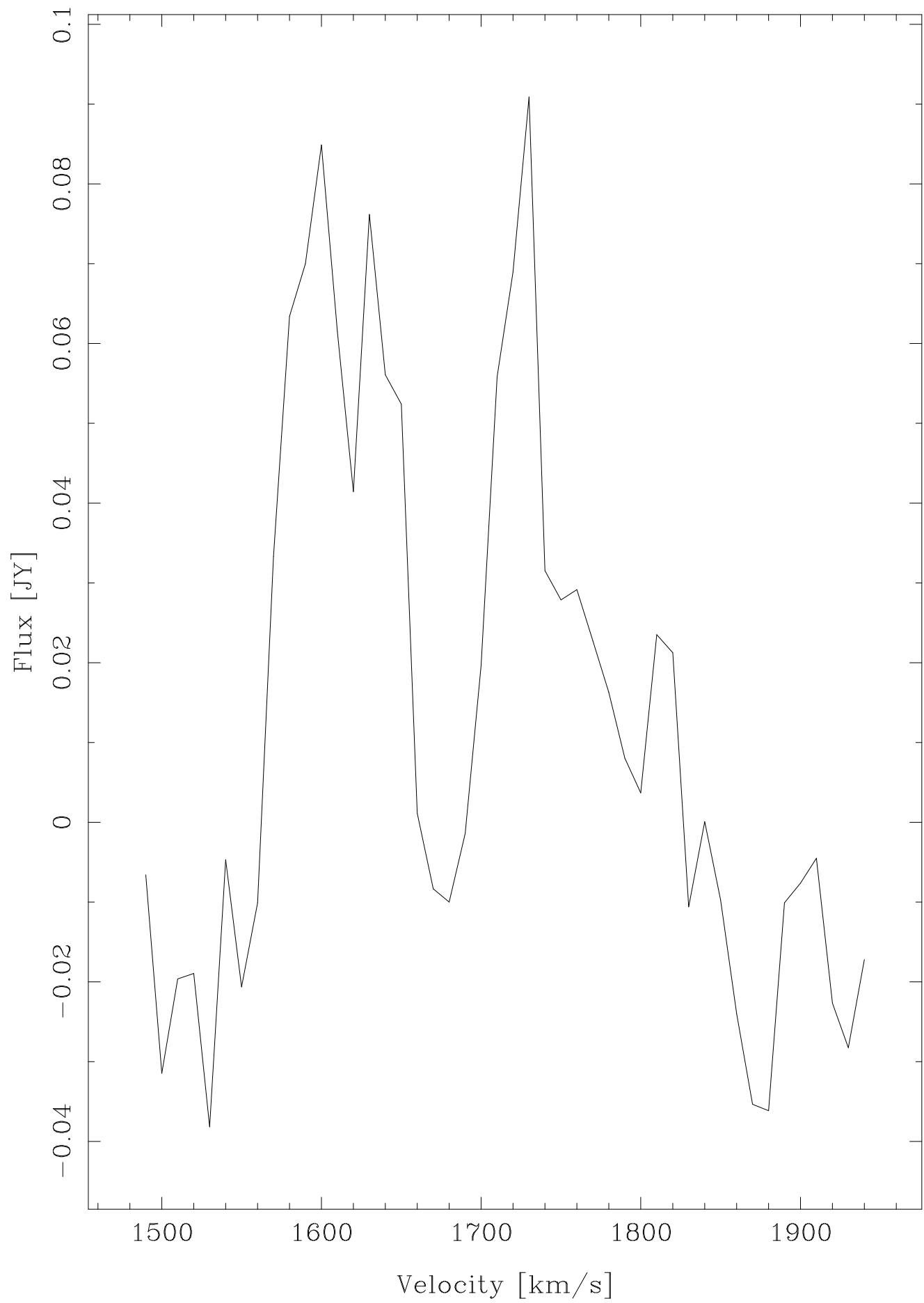


This figure "J1007.dss.HI.gif" is available in "gif" format from:

<http://arxiv.org/ps/astro-ph/0211391v1>

This figure "ic2554.1413.gif" is available in "gif" format from:

<http://arxiv.org/ps/astro-ph/0211391v1>



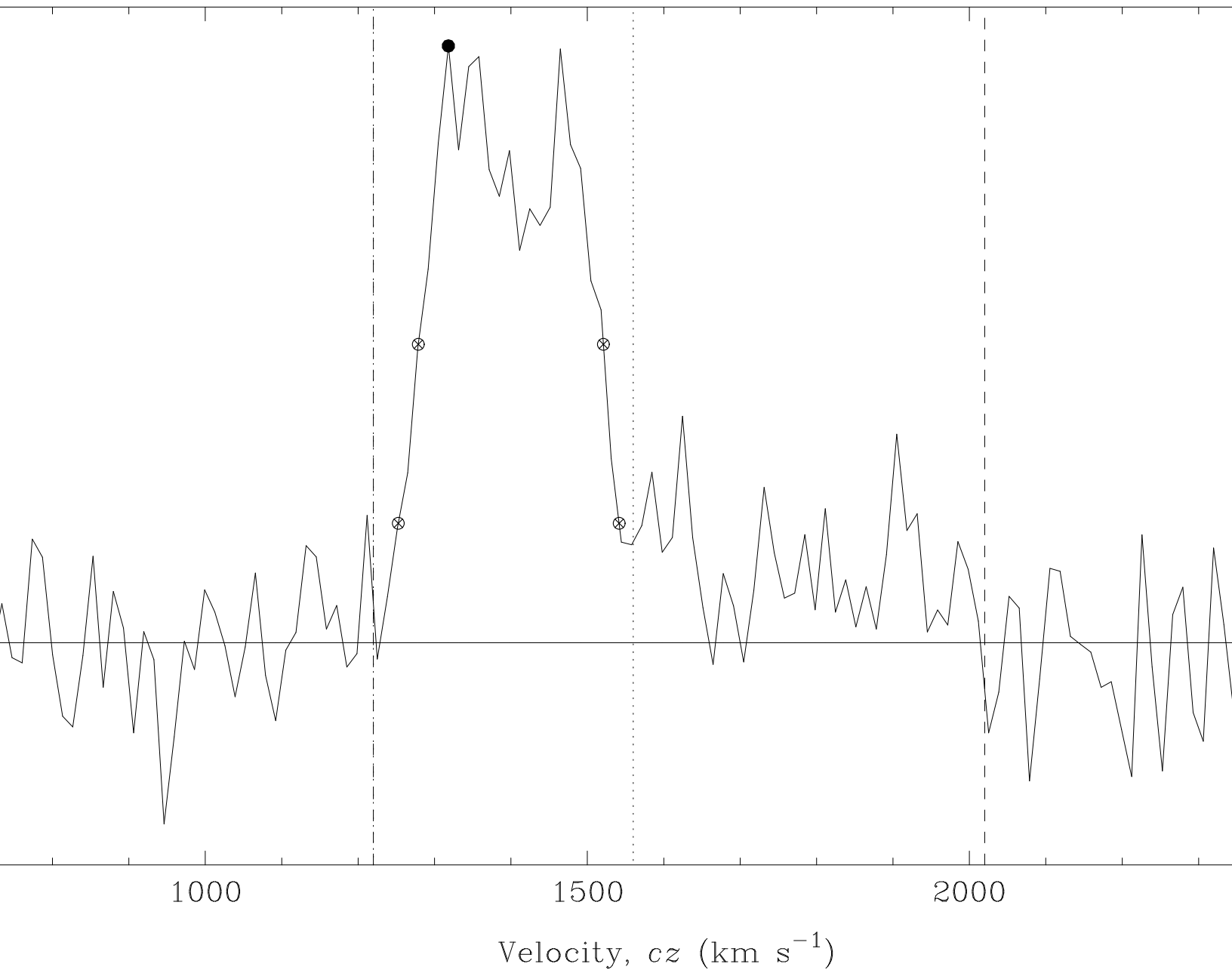
This figure "ic2554.2496.gif" is available in "gif" format from:

<http://arxiv.org/ps/astro-ph/0211391v1>

This figure "IC2554_dss.gif" is available in "gif" format from:

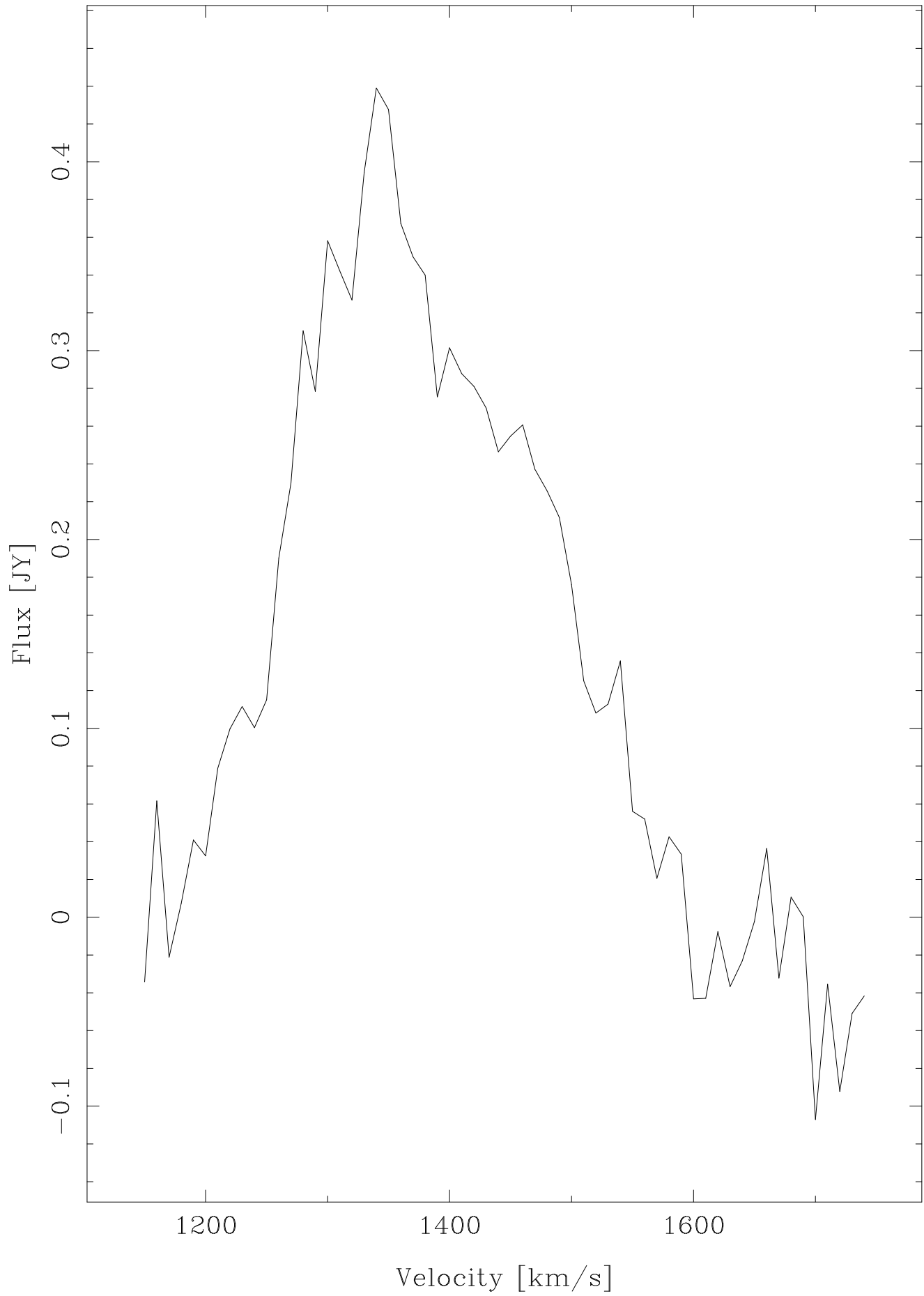
<http://arxiv.org/ps/astro-ph/0211391v1>

Object:
Requested: 10:08:50.00 -67:01:52.00
Actual : 10:08:50.00 -67:01:52.00
Quinox : J2000



This figure "ic2554_laustsen.crossbar.gif" is available in "gif" format from:

<http://arxiv.org/ps/astro-ph/0211391v1>



This figure "ic2554.4800.gif" is available in "gif" format from:

<http://arxiv.org/ps/astro-ph/0211391v1>

This figure "ic2554.HIJ1007-6659.gif" is available in "gif" format from:

<http://arxiv.org/ps/astro-ph/0211391v1>

This figure "ic2554.8640.gif" is available in "gif" format from:

<http://arxiv.org/ps/astro-ph/0211391v1>

